ELASTIC PROPERTIES OF Cr-Mo ALLOYED SINTERED STEELS: A COMPARISON OF DYNAMIC AND STATIC YOUNG'S MODULI

M. Azadbeh, Ch. Gierl, H. Danninger

Abstract

Under service conditions, P/M sintered parts are frequently subjected to mechanical loads. Their behaviour under such loading conditions is therefore of considerable importance. The design of gears and other mechanical components requires knowledge of Young's modulus to calculate the stresses at the point of contact. The Young's modulus (E) allows engineers and scientists to calculate the behaviour of a material under load. This paper reports a study on Young's modulus of Cr-Mo prealloyed sintered steels of varying porosity. E was determined by a non-destructive technique using ultrasonic waves and for comparison by static - tensile – testing. It was found that measuring the dynamic Young's modulus is easier than the static one; however also the latter can be reliably measured if testing is carefully done. The values for E_{stat} are slightly lower than for E_{dyn}. There is a virtually linear relationship between density and Young's modulus for both 1.5% Cr and 3% Cr steels, the effect of the Cr content being marginal.

Keywords: sintered steels, Cr prealloyed steels, Young's modulus, sintered density, non-destructive test.

INTRODUCTION

Sintered ferrous powder metallurgy (P/M) components have emerged as attractive candidates for replacing parts from wrought steels in many applications, due to their low cost, high performance, and ability to be processed to net or at least near-net shape. Sintered materials are typically characterized by residual porosity after sintering, which is quite detrimental to the mechanical properties of these materials [1-9]. Porous alloys, produced by powder metallurgy, are characterized by a heterogeneous microstructure, with the presence of pores and in part also complex matrix microstructure. Pores, in particular, act as stress and strain concentrators reducing strength and ductility [10]. During tensile testing, the deviation from linearity in the stress-strain curve starts very early due to development of microplastic regions at the pore necks at low applied stress [8], rendering measurement of the Young's modulus in static tests rather tricky. The plastic regions spread in the matrix and may induce a pore volume growth, with a corresponding decrease in the effective load-bearing section [11, 12]. In addition, depending on the pore irregularity and matrix deformability, microcracks induce an accumulation of damage in the microstructure, which ultimately may lead to fracture [13].

More than 80% of structural P/M parts are used for automobile applications. During the actual service conditions, cyclic stresses on the parts commonly remain within the proportional limit. So the mainly required characteristics of these parts are high fatigue

Maziyar Azadbeh, Christian Gierl, Herbert Danninger, Institute of Chemical Technologies and Analytics, Vienna University of Technology Getreidemarkt 9/164, A-1060 Wien/Vienna, Austria

strength and high Young's modulus. The design of gears and other mechanical components requires knowledge of Young's modulus and Poisson's ratio to calculate the stresses at the point of contact.

The Young's modulus allows engineers to calculate the behaviour of a material under load. The modulus of elasticity is a mechanical property the determination of which does not involve plastic deformation of specimen volume [14]. Advanced finite element simulation and computer-aided design techniques require prior knowledge of elastic properties for PM parts. Thus, determining elastic properties of sintered metals becomes critical. Non-destructive characterization techniques have emerged as promising means of evaluating these properties [15,16].

In the case of obtaining Young's modulus from tensile tests, care must be taken not to locally induce plastic deformation. Tensile testing experiments would generate local strains of a few percent in the neck regions. These are small, but exceed the yield stress of the matrix material. This suggests that the stress-strain curves for the nominally elastic region of such materials should be non-reversible. Therefore, measuring Young's modulus at significantly lower stresses, and thus in the definitely elastic range, is preferable. This is possible by using ultrasonic resonance methods, which operate at low stress amplitudes and thus far from any stress that might result in microplastic deformation [17,18].

EXPERIMENTAL PROCEDURE

Rectangular test specimens, 100 x 12 x 8 mm^3 in size were produced from prealloyed Astaloy CrM and Astaloy CrL powders, (Höganäs AB, Sweden), with 0.5 and 0.6 wt% natural graphite C-UF4, respectively, and 0.6 wt% HWC as lubricant. Compaction was carried out uniaxially in a pressing tool with floating die, and five compacting pressures were chosen (250, 400, 500, 600, 700 MPa) to obtain materials with different density levels. The green bodies were sintered at three different temperatures (1120°C, 1250°C, 1300°C). Sintering at 1120°C was carried out in a laboratory furnace with gas-tight superalloy retort in flowing high purity nitrogen (5.0 grade = min. 99.999 purity, flow rate 2 l/min). To prevent sticking of the samples together, they were put in steel boxes filled with alumina powder. Delubing of these samples was accomplished in a small laboratory furnace at 600°C for 30 min, and then the boat was pushed into the exit zone. After cooling, the boat was transported into the high temperature zone of the larger furnace and remained there for 60 minutes. For sintering at higher temperatures (1250°C and 1300°C), a pusher furnace with Mo heating coil on an alumina muffle (Degussa type "Baby" furnace) was used. To ensure reasonably clean atmosphere, the sintering was done in steel boxes filled with a mixture of 50 wt% Al_2O_3 and 50 wt% Fe-8Al as getter material. Delubing of these samples was done in the preheating zone for 25 minutes, and then the boat remained in the high temperature zone for 60 minutes. After sintering in H_2, the boat was pushed into the water-jacketed exit zone.

Densities of green compacts were determined from measurements of the mass and the dimensions of the compacts, while those of the sintered compacts were determined using Archimedes principle (DIN ISO 3369).

The dynamic Young' modulus, E_{dyn}, was determined using a resonance system, as shown below, and evaluated according to ASTM E 1876-99. The arrangement of the instrumentation is shown in Fig.1. It consists of an impulser, a suitable pickup transducer to convert the mechanical vibration into an electrical signal, an electronic system consisting of a signal conditioner/amplifier, a signal analyser, a frequency readout device, and a support system.

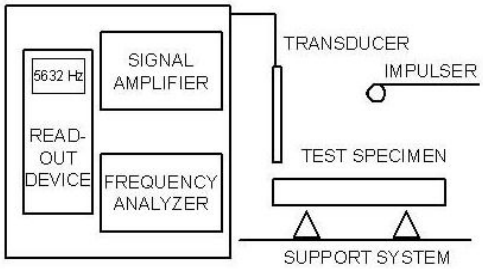

Fig.1. Block diagram of a typical test apparatus for dynamic Young's modulus.

The resultant frequency reading was recorded, and the test was repeated until five consecutive values were obtained that differed < 1% of each other. The mean value of these five readings was used to determine the fundamental resonant frequency. By use of these data the dynamic Young's modulus for a rectangular bar can be calculated from the following equation:

$$E=0,9465(mf_f^2/b)(L^3/t^3)T_1 \quad (1)$$

where:

E = Young's modulus, Pa
M = mass of the bar, g
B = width of the bar, mm
L = length of the bar, mm
T = thickness of the bar, mm
f_f = fundamental resonant frequency of bar in flexure, Hz
T_1 = correction factor. If $L/t \geq 20$, T_1 can be calculated from the following equation:

$$T_1 = [1.000+6.585\ (t/L)^2] \quad (2)$$

Edge treatments such as chamfers or radii are not considered in the analytical equations.

Edge chamfers change the resonant frequency of the test bars and introduce error into the calculations of the dynamic modulus. It is recommended that specimens for this test method not have chamfered or rounded edges [15]. The specimens shall be prepared so that they are either rectangular or circular in cross section. All surfaces on the rectangular specimen shall be flat. Opposite surfaces across the length, thickness and width shall be parallel to within 0.1%. Specimen mass shall be determined to within 0.1%. Specimen length shall be measured to within 0.1%. The thickness and width of the rectangular specimen shall be measured to within 0.1% at three locations and an average determined.

To have proper samples, two ends of the samples were cut and then machined. To ensure reasonably flat surfaces, all sides of samples were wet ground with SiC paper with different mesh size (180, 320, 600, 1000 mesh). Then the samples were dried at 110°C for 60 min to remove any water from the pores.

Static Young's modulus measurements were done under tensile loading at room temperature on the same samples using a Zwick 1474 universal testing machine with Messphysik optical extensometer, the maximum applied stress being 100, 110, 140, 150, 150 MPa, respectively, for the samples that were compacted at 250, 400, 500, 600, 700 MPa . The gauge length of the extensometer used was 12.5 mm. The static modulus was determined from the linear regression of the stress-strain graphs within this range. A tensile test was first used to determine the elastic limit of the sintered materials, since

determination of static Young's modulus without any idea of the results expected is not easy to do and may introduce damage to the samples. The crosshead speed was the same for all tested samples (2 mm/min).To compare dynamic and static Young's moduli, these tests were done on the same samples (first dynamic testing and then static testing were done).

RESULTS AND DISCUSSION

The data obtained as results of the experiments are presented in Table 1, and for better comparison are also shown graphically, in Figs.2 and 3.

Tab.1. Influence of the compacting pressure on sintered density and Young's modulus.

Compacting Pressure [MPa]		Sintered Density [g/cm^3]			Dynamic Young's Mod. [GPa]			Static Young's Modulus [GPa]		
		Sintering Temperature			Sintering Temperature			Sintering Temperature		
		1120°C	1250°C	1300°C	1120°C	1250°C	1300°C	1120°C	1250°C	1300°C
Ast CrM +0.5C	250	5.91	6.01	6.14	84	95	104	82	93	102
	400	6.50	6.60	6.68	120	130	137	118	128	134
	500	6.73	6.82	6.90	133	145	150	132	142	148
	600	6.90	6.99	7.07	147	155	160	145	152	158
	700	7.01	7.12	7.18	155	162	167	149	157	165
Ast CrL +0.6C	250	6.11	6.21	6.35	95	102	117	90	97	115
	400	6.67	6.74	6.87	130	137	150	127	134	146
	500	6.85	6.94	7.04	143	152	160	140	148	153
	600	7.02	7.11	7.17	155	163	168	152	156	160
	700	7.12	7.21	7.26	165	173	178	159	163	168

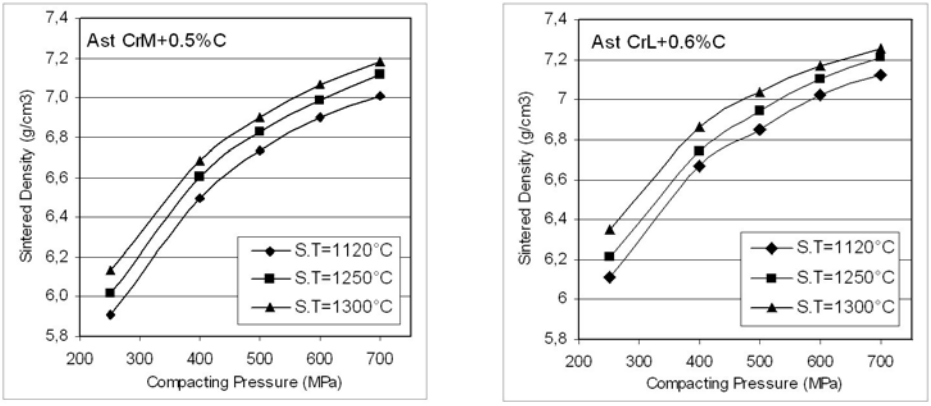

Fig.2. Comparison of sintered density for Astaloy CrM-C and Astaloy CrL-C for different sintering temperatures and compacting pressures.

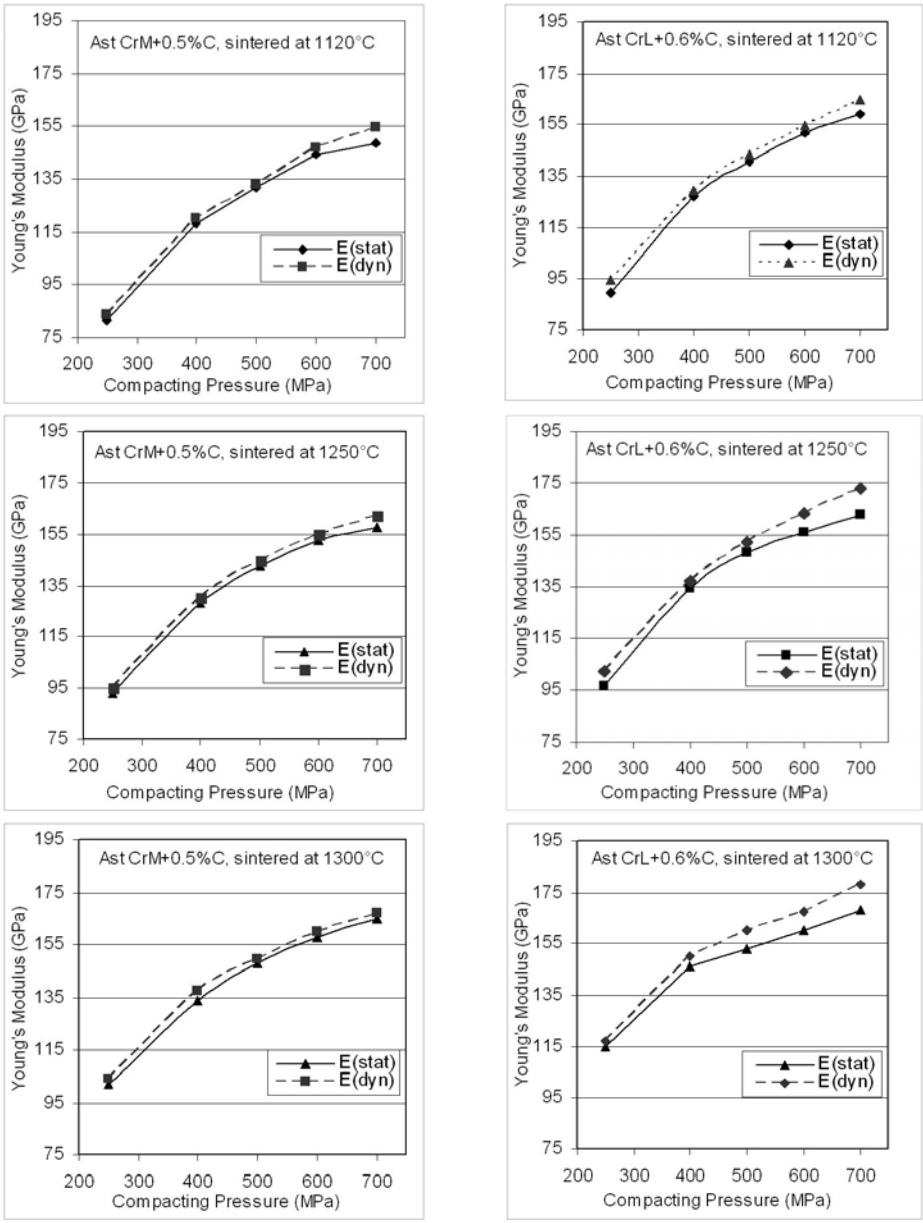

Fig.3. Dynamic and static Young's modulus vs. compacting pressure for Astaloy CrM +0.5%C and Astaloy CrL+0.6%C sintered at different temperatures.

Regarding the density values, it stands out clearly that the green and sintered density of the Astaloy CrM specimens is lower than that of the Astaloy CrL based ones, which is attributable to the lower compactibility of the higher alloyed steel as a consequence of solid solution hardening. With both materials the sintered density tends to increase at higher sintering temperature, as shown in Fig.2. This trend is still more visible

from the dimensional change: here, at higher sintering temperature (1300°C) both materials exhibit markedly more shrinkage than at lowers sintering temperature (1120°C).

In Figure 3 the dynamic and static Young's moduli of the specimens are plotted as a function of compacting pressure and sintering temperature. The results show the progressive increase of the Young's modulus with higher compacting pressure, but the slope of the graphs gradually decreases in a very similar way as does the density (see Fig.2).

If Astaloy CrL and CrM are compared, at the same sintered density both materials show almost the same value of the dynamic Young's Modulus (e.g: E_{dyn} of CrM with 7.18 g/cm^3 is 167 GPa and E_{dyn} of CrL with 7.17 g/cm^3 is 168 GPa).

With increasing sintering temperature, the dynamic Young's modulus increases at every compaction pressure. The phenomenon is due to the fact that with higher sintering temperature the pores will spheroidize, their surface becomes smooth, and as a result the load bearing cross section gets higher which also contributes to this effect. At lower compacting pressure the effect of increasing sintering temperature on the Young's modulus is more pronounced than at higher pressure.

The above figure (Fig.3) compares the Young's moduli obtained from static testing (tensile test) with those calculated from resonance frequency measurements. While the values for the dynamic and static measurements agree quite well, the dynamic measurements are always slightly higher, as shown in Table 2. It seems that the difference increases with the density [19], and for Astaloy CrL the difference is slightly larger than for CrM. In principle, there should be always a slight difference between both moduli, E_{dyn} being higher due to physical reasons: E_{dyn} is measured in an adiabatic process and E_{stat} in an isothermal one. The difference can be expected to be in the range of 3%, which is in good agreement with the results obtained here.

Tab.2. Ratio between dynamic and static Young's moduli for differently compacted and sintered Astaloy CrM-0.5%C and Astaloy CrL-0.6%C.

Compacting Pressure [MPa]		Sintered Density [g/cm^3]			Ratio E(dyn.)/E(stat.)		
		Sintering Temperature [°C]			Sintering Temperature [°C]		
		1120	1250	1300	1120	1250	1300
Astaloy CrM	250	5.91	6.01	6.14	1.024	1.022	1.020
	400	6.50	6.60	6.68	1.017	1.016	1.022
	500	6.73	6.82	6.90	1.008	1.021	1.014
	600	6.90	6.99	7.07	1.014	1.020	1.013
	700	7.01	7.12	7.18	1.040	1.032	1.012
Astaloy CrL	250	6.11	6.21	6.35	1.056	1.052	1.017
	400	6.67	6.74	6.87	1.024	1.022	1.027
	500	6.85	6.94	7.04	1.021	1.027	1.046
	600	7.02	7.11	7.17	1.020	1.045	1.050
	700	7.12	7.21	7.26	1.038	1.061	1.060

The Young's modulus is determined by means of sonic or ultrasonic methods [20-22] in order to induce low strains and thus ascertain that the applied stress is lower than σ_N (see Fig.1 in [22]). When using tensile testing, the true static Young's modulus is difficult to determine, and if the deviation from linearity starts very early and gradually, as typical for porous sintered steels, or if the sensitivity of the adopted strain gage is low, a too low value for the modulus is actually measured. As stated above, local plasticity at the pore edges during tensile testing causes the occurrence of localized yielding well below general

yielding in porous alloys which results in a stress-strain graph within the nominally elastic range that is in fact curved rather than linear.

The influence of sintering temperature on dynamic Young's modulus is shown in Fig.4. It can be seen that the sintering temperature is decidedly affecting Young's modulus. A pronounced influence of the sintering temperature can be noticed in the lower compacting pressure ranges, since at lower compacting pressure the increase of Young' modulus with rising sintering temperature is more pronounced than at higher pressure (as also visible in this Figure). The effect is ascribed to the progressive rounding of the pores and increasing load bearing cross section.

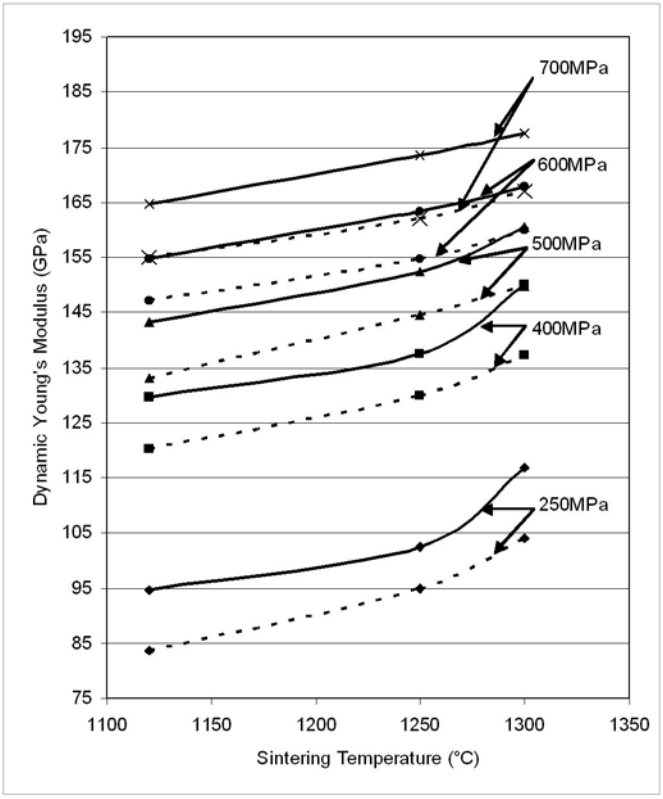

Fig.4. Dynamic Young's modulus vs. sintering temperature at different compaction pressures for Astaloy CrM+0.5%C and Astaloy CrL+0.6%C. (Solid line …CrL, broken line…CrM).

It can also be seen that there is quite a difference between sintering at 1250 and 1300°C, respectively, in particular in the low density range.

Figure 5 shows the dynamical (resonance frequency measured) Young's modulus as a function of the sintered density for Astaloy CrM+0.5%C and Astaloy CrL+0.6%C, respectively. There is a linear relationship between dynamic Young's modulus and sintered density; as can be seen, the Young's modulus increases at a constant rate with increasing sintered density. A linear regression correlation was performed for the results obtained for these two materials (Fig.6), and excellent correlation with a correlation coefficient of $R^2 = 0.9891$ was recorded.

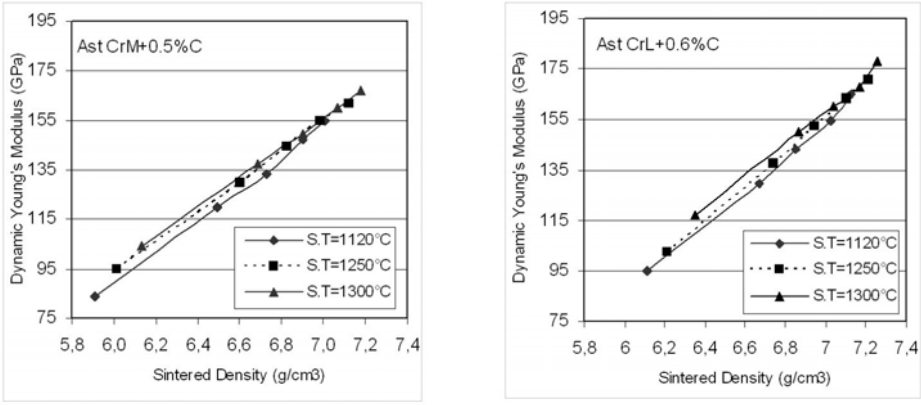

Fig.5. Dynamic Young's modulus as a function of the density for Astaloy CrM+0.5%C and Astaloy CrL+0.6%C.

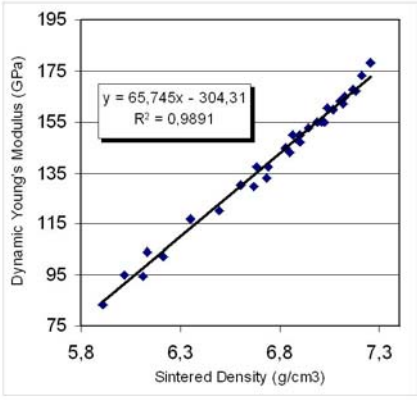

Fig.6. Linear regression correlation for dynamic Young's modulus vs. sintered density (data for both Astaloy CrL and CrM).

$$E_{dyn} = 65.745\ \rho_s - 304.31 \quad (3)$$

The above technique for E_{dyn} can be used to measure resonant frequencies e.g. for the purposes of quality control and acceptance of test specimens of both regular and complex shapes. A range of acceptable resonant frequencies is determined for a specimen with a particular geometry and mass.

It can be concluded that the influence of alloying chromium (up to 3%) on the Young's modulus of ferrous sintered materials is very small. The same conclusions were also reported for the alloying elements (Cu, C, Ni, Mo, Cr) [23] when using the resonance method.

The results of static Young's modulus for Astaloy CrM+0.5%C and Astaloy CrL+0.6%C at different sintered densities is shown in Fig.7. Also the static Young's modulus increases linearly with increasing sintered density. As can be seen, both materials show a linear relationship between static Young's modulus and sintered density at each sintering temperature (1120, 1250, 1300°C), and these 3 graphs virtually coincide.

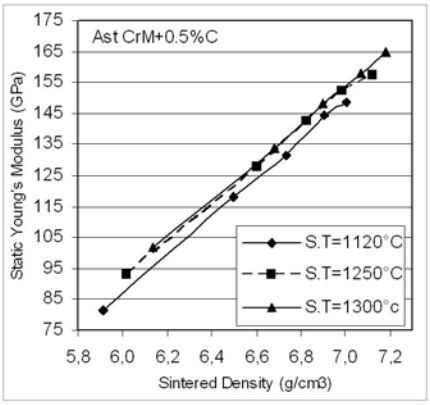

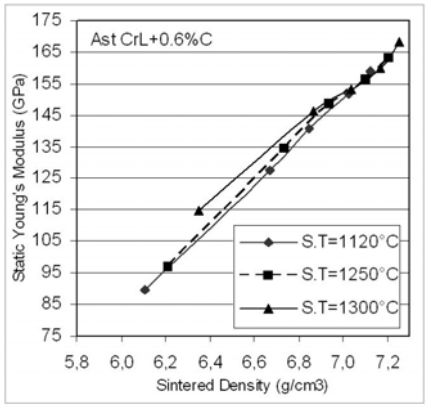

Fig.7. Static Young's modulus vs. sintered density for AstaloyCrM +0.5%C and AstaloyCrL+0.6%C.

There is also a linear relationship between static Young's modulus and sintered density; as can be seen in Figure 8, the static Young's modulus increases at a constant rate with increasing sintered density. Two linear regression correlations were performed separately for the results obtained for Astaloy CrM+0.5%C and Astaloy CrL+0.6%C, and excellent correlation with correlation coefficients $R^2 = 0{,}991$ and $R^2 = 0{,}989$ respectively for Astaloy CrM and Astaloy CrL were recorded. In parallel, analysis of all calculated data for static Young's modulus of Astaloy CrM+0.5%C with Astaloy CrL+0.6%C was performed, and the result is shown in Fig.9. A linear regression correlation was performed for the results obtained for these two materials, and excellent correlation with a correlation coefficient $R^2 = 0.9879$ was recorded. This confirms that the effect of the Cr content – 1.5% or 3.0% - on the Young's modulus is marginal.

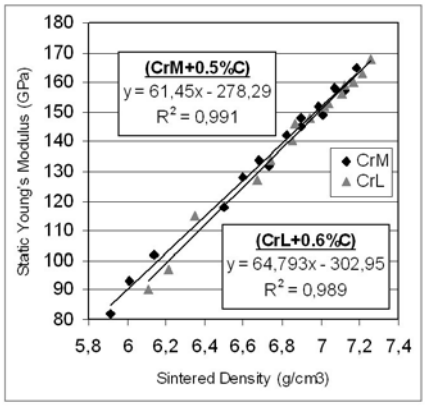

Fig.8. Comparative linear regression correlation for static Young's modulus of Astaloy CrM-C and Astaloy CrL-C vs. sintered density for all sintering temperatures.

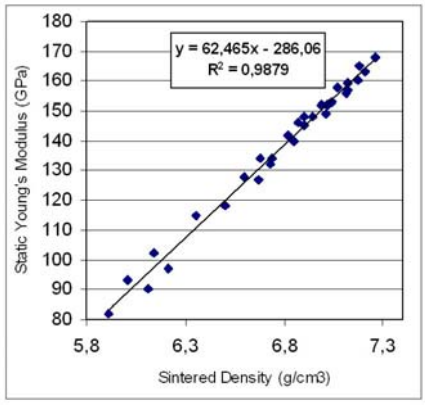

Fig.9. Linear regression correlation for static Young's modulus (all data) vs. sintered density.

CONCLUSIONS

For determining the Young's modulus of porous sintered steels prepared from Cr-Mo prealloy powders, a resonance test method has been used. This technique is very fast and reliable compared to static measurement of E in tensile testing, in the latter case too low values being easily obtained due to the onset of microplasticity well below the nominal yield stress. However, by careful testing also for the static Young's modulus reliable data have been obtained.

The dynamic Young's modulus obtained by resonance techniques is slightly higher than the static modulus, due to physical reasons. Allowing for this difference, both sets of data are in very good agreement.

Both compacting pressure and sintering temperature affect the E values measured; if however the effect of both parameters on the density is regarded, it can be shown that both E_{dyn} and E_{stat} are linearly correlated to the sintered density. The equations for this relationship hold both for the 1.5% Cr and the 3% Cr materials, confirming that this difference in the composition does not noticeably affect the Young's modulus of the matrix.

Acknowledgement

The authors would like to thank Högänas AB, Sweden, for supplying the starting powders used, and Prof. B. Weiss and Dr G. Khatibi, University of Vienna, for assistance with E_{dyn} testing.

REFERENCES

[1] Šalak, A.: Ferrous Powder Metallurgy. Cambridge : Cambridge International Science Publishing, 1997
[2] Hadrboletz, A., Weiss, B.: Int. Mater. Rev., vol. 42, 1997, p. 1
[3] Chawla, N., Polasik, SJ., Narasimhan, KS., Koopman, M., Chawla, KK.: Int. J. Powder Metall., vol. 37, 2001, p. 49
[4] Chawla, N., Murphy, TF., Narasimhan, KS., Koopman, M., Chawla, KK.: Mater. Sci. Eng. A, vol. 308, 2001, p. 180
[5] Polasik SJ., Williams, JJ., Chawla, N.: Metall. Trans. A, vol. 33, 2002, p. 73
[6] Chawla, N., Jester, B., Vonk, DT.: Mater. Sci. Eng. A, vol. 346, 2003, p. 266
[7] Haynes, R.: The Mechanical Behaviour of Sintered Metals. London : Freund, 1981
[8] Eudier, M.: Powder Metall., 1962, p. 278
[9] Šalak, A. et al.: Powder Metall. Int., vol. 6, 1974, p. 128
[10] German, RM.: Powder Metallurgy Science. 2nd ed. Princeton : Metal Powder Industries Federation, 1994
[11] Griffiths, TJ., Davis, R., Bassett, MB.: Powder Metallurgy, vol. 22, 1979, p. 119
[12] Spitzig, WA., Smelser, RE., Richmond, O.: Acta Metall., vol. 36, 1988, p. 1201
[13] Straffelini, G., Molinari, A.: Materials Science and Engineering A, vol. 334, 2002, p.96
[14] Karlsson, B., Bertilsson, I.: Scand. J. Metallurgy, vol. 11, 1982, p. 267
[15] ASTM E 1876-99
[16] Phillips, RR., Franciscovich, W.: Progr. Powder Metallurgy, vol. 39, 1983, p. 369
[17] Moon, JR.: Powder Metall., vol. 32, 1989, no. 2, p. 132
[18] Leheup, ER., Moon, JR.: Powder Metall., 1980, no. 1, p. 15
[19] Yu, CJ., Prucher, T.: Adv. Powder Metall. & Partic. Mater., vol. 1, 1993, p. 273
[20] Haynes, R., Egediege, JT.: Powder Metall., vol. 32, 1989, p. 47
[21] Griffiths, TJ., Ghanizadeh, A.: Powder Metall., vol. 29, 1986, p. 129
[22] Straffelini, G., Fontanari, V., Molinari, A.: Mater. Sci. Eng. A, vol. 260, 1999, p. 197
[23] Haung, H., Fujiki, A., Yang, J., Goto, JM., Watanabe, T. In: Proc. 2000 Powder Metallurgy World Congress, Kyoto. Ed. K. Kosuge. Vol. 2. Tokyo : JPMA, p. 1598